Translational Oncology 68 (2026) 102775

Contents lists available at ScienceDirect

Translational Oncology

journal homepage: www.elsevier.com/locate/tranon

Original Research

Transcriptomic and single-cell analyses reveal the prognostic value of ETV4 and its role in shaping the immune landscape of colorectal cancer

Ruipeng Meng [1], Shilong Wang [1], Zhanfei She, Huaiming Wang, Bo Wu, Yu Qiao, Pengyuan Chen, Nargerel, Xiaofeng Yang, Liang Wang [*]

Department of General Surgery, Ordos Central Hospital Affiliated to Inner Mongolia Medical University, Ordos, Inner Mongolia, 017010, China

ARTICLE INFO

Keywords:
ETV4
Colorectal Cancer
M2 Macrophage
WNT/β-catenin signaling

ABSTRACT

Background: Colorectal cancer (CRC) remains a major health threat with poor prognosis in advanced stages. The transcription factor ETV4 (ETS translocation variant 4) has been implicated in various cancers, but its specific role, prognostic value, and mechanisms in CRC, particularly concerning the tumor immune microenvironment, are not fully understood.

Methods: We performed a comprehensive analysis using transcriptomic data from The Cancer Genome Atlas (TCGA) and single-cell RNA sequencing data from the GEO database (GSE231559). Bioinformatic approaches included survival analysis, immune cell infiltration estimation via CIBERSORT, gene set enrichment analysis (GSEA), gene set variation analysis (GSVA), and single-cell clustering. Experimental validation was conducted on clinical CRC tissue samples and HCT-116 cells, employing flow cytometry, immunohistochemistry, quantitative real-time PCR (Q-PCR), and Western blot.

Results: In the TCGA cohort, ETV4 was significantly upregulated in 650 CRC tissues vs 51 adjacent normal tissues, with high expression linked to poorer overall survival in CRC patients.Immune infiltration analysis revealed correlations between ETV4 expression and specific immune cell subsets, notably macrophages. Flow cytometry and immunohistochemistry confirmed that high ETV4 expression was linked to increased polarization of immunosuppressive M2-type macrophages in the tumor microenvironment. Furthermore, bioinformatic GSVA and subsequent wet-lab experiments demonstrated that ETV4 is a downstream target gene of the *WNT/β-catenin* signaling pathway. Activation of this pathway upregulated ETV4 expression, while inhibition downregulated it, establishing a functional link.

Conclusion: This integrative study reveals that ETV4 is a prognostic biomarker in CRC. It promotes tumor progression by reshaping the immunosuppressive microenvironment, particularly through inducing M2 macrophage polarization, and is regulated by the oncogenic *WNT/β-catenin* pathway. These findings suggest that ETV4 is expected to become a potential diagnostic biomarker and candidate therapeutic target for colorectal cancer, providing a novel direction for subsequent research on the diagnosis and treatment of CRC.

Introduction

Altered dietary habits and the rising trend of obesity have established Colorectal Cancer (CRC) as a prevalent and serious threat to human health, with its incidence and mortality rates increasing annually [1]. Cancer statistics indicate that the incidence of CRC in China has surged nearly fivefold over the past three decades [2]. The rising proportion of cases in individuals under 50 years old presents significant challenges for early detection and treatment, underscoring an urgent need to identify novel diagnostic and therapeutic targets for CRC.

In recent years, immunotherapy has markedly improved patient prognosis [3]. Its core mechanism involves activating or enhancing the immune system to recognize and attack cancer cells, where immune checkpoints such as CTLA-4 and PD-1/PD-L1 play a crucial role [4], offering hope for patients with high microsatellite instability (MSI-H) CRC. The tumor immune microenvironment (TME), the local milieu in

* Corresponding author at: Department of General Surgery, Ordos Central Hospital Affiliated to Inner Mongolia Medical University, Ordos, Inner Mongolia, 017010, China.
E-mail address: 120803737@qq.com (L. Wang).
[1] These authors contributed equally to this work as co-first authors.

https://doi.org/10.1016/j.tranon.2026.102775
Received 23 January 2026; Received in revised form 31 March 2026; Accepted 13 April 2026

which tumor cells survive, directly influences whether immune checkpoint inhibitors (ICIs) can effectively activate the immune system. This influence is mediated by the TME's immune composition, molecular features, and metabolic state [5,6]. Within the TME, tumor-associated macrophages (TAMs) play a significant role in CRC metastasis [7], are associated with poor prognosis and drug resistance, and thus represent an ideal therapeutic target for CRC [8].

ETV4 (ETS translocation variant 4) is a member of the ETS (E26 transformation-specific) transcription factor family and exerts transcriptional regulatory functions in the development and progression of various cancers [9]. Its expression is also closely associated with immune cell infiltration, mismatch repair gene expression, and DNA methylation [10]. Although existing studies have reported that ETV4 is highly expressed in CRC and correlated with poor prognosis, its specific role in the tumor immune microenvironment (TIME) of CRC has not been fully elucidated. Specifically, it remains unclear whether ETV4 regulates the infiltration and polarization of immune cells (such as macrophages) in CRC, and the association between ETV4 and key signaling pathways related to CRC progression (such as the *WNT/β-catenin* pathway) has not been systematically investigated. Therefore, this study aims to explore the role of ETV4 in CRC, clarify its association with the tumor immune microenvironment and the *WNT/β-catenin* pathway, and provide novel insights for the diagnosis and treatment of CRC.

Materials and methods

Data acquisition and processing

Processed gene expression data for colorectal cancer were downloaded from The Cancer Genome Atlas (TCGA) database (https://portal.gdc.cancer.gov/). The dataset included samples from a normal control group ($n = 51$) and a tumor group ($n = 650$). Single-cell RNA sequencing data files for the GSE231559 dataset were obtained from the Gene Expression Omnibus (GEO) database (https://www.ncbi.nlm.nih.gov/geo/), comprising expression profiles from 9 patients.

Co-expression analysis

To investigate the co-expression network of the ETV4 gene in colorectal cancer, a co-expression analysis was performed. Genes with an absolute Pearson correlation coefficient > 0.65 and a p-value < 0.05 were considered significantly co-expressed with ETV4. Following the screening of genes most significantly associated with ETV4 expression, correlation circle plots and heatmaps were generated using the R packages "corrplot" and "circlize".

Immune cell infiltration analysis

The relative proportions of 22 types of tumor-infiltrating immune cells were estimated from the RNA-seq data of CRC patients using the CIBERSORT algorithm. Subsequently, correlation analyses were conducted between ETV4 gene expression levels and the estimated immune cell fractions. A p-value < 0.05 was considered statistically significant.

Gene set enrichment analysis (GSEA) and gene set variation analysis (GSVA)

Patients were stratified into high and low ETV4 expression groups based on the median expression value. GSEA was then employed to identify signaling pathways differentially enriched between these two groups. The Molecular Signatures Database (MsigDB) version 7.0 annotated gene sets served as the reference for pathway analysis. Significantly enriched gene sets (adjusted p-value < 0.05) were ranked according to their normalized enrichment score (NES). For GSVA, gene sets were obtained from the Molecular Signatures Database. The GSVA algorithm was applied to calculate an enrichment score for each gene set per sample, thereby evaluating the potential variation in biological functions across different samples.

Quality control of single-cell RNA sequencing data

The single-cell expression matrix was processed using the Seurat package. Initial cell filtration was based on three metrics: the total UMI counts per cell, the number of genes detected per cell, and the percentage of mitochondrial gene expression (calculated as the total expression of mitochondrial genes divided by the total expression of all genes). Cells with a high mitochondrial gene percentage, indicative of low RNA content and likely undergoing apoptosis or are of low quality, were removed. Quality control was further performed using the Median Absolute Deviation (MAD). Any cell for which a metric deviated >3 median absolute deviations from the median was considered an outlier and filtered out. Potential doublets (multiple cells captured within a single droplet) were identified and removed using the DoubletFinder software (v2.0.4) for each sample individually, thereby completing the cell quality control process.Quality control index filtering thresholds: To avoid bias caused by fixed thresholds, the median absolute deviation (MAD) statistical method was used for cell filtration in this study. The specific criteria were as follows: cells with the number of detected genes (nFeature_RNA) ≥ 200 and within the range of median $\pm$ 3-fold MAD were retained; cells with total UMI counts (nCount_RNA) within the range of median $\pm$ 3-fold MAD were retained; cells with mitochondrial gene ratio (percent.mt) $\leq$ median + 3-fold MAD were retained.Potential doublets (multiple cells captured within a single droplet) were identified and removed using the DoubletFinder software (v2.0.4) for each sample individually, thereby completing the cell quality control process.

Dimensionality reduction, clustering, and annotation of single-cell RNA sequencing data

Normalization was performed using the global-scaling "LogNormalize" method, which scales the total expression for each cell to 10,000, followed by log-transformation. Cell cycle scores were calculated using the CellCycleScoring function. Highly variable features were identified using FindVariableFeatures. The ScaleData function was applied to regress out unwanted sources of variation, primarily stemming from the percentage of mitochondrial gene expression and UMI counts. Principal Component Analysis (PCA) was conducted for linear dimensionality reduction, and significant principal components were selected for downstream analysis. Basis for selection of single-cell analysis parameters: The number of principal components for PCA was determined by Elbow Plot. By observing the inflection point of the variance interpretation rate of principal components, the first 20 principal components were selected for subsequent UMAP dimensionality reduction, cell clustering and other analyses. The principal components selected at this time can cover most of the biological differences in the data, and the clustering results are stable and repeatable. The Harmony algorithm was used to integrate data and remove batch effects. For visualization and non-linear dimensionality reduction, Uniform Manifold Approximation and Projection (UMAP) was performed. Cell type annotation was carried out primarily by querying known cell markers from the CellMarker and PanglaoDB databases and referencing relevant literature, with automated annotation provided by the SingleR software serving as a supplementary guide.

Flow cytometry and immunohistochemistry (IHC)

Tumor tissues (CA group, $n = 40$) and paired adjacent normal colorectal tissues (NOR group, $n = 40$) were collected from 40 CRC patients who underwent surgical resection at our hospital. All samples were pathologically confirmed, and the patients had not received any preoperative anti-tumor interventions such as radiotherapy,

chemotherapy, or immunotherapy. Upon collection, samples were immediately processed for flow cytometry analysis or fixed for paraffin-embedded tissue block preparation for IHC.

For flow cytometry, the following antibodies from BioLegend were used: Alexa Fluor® 488 anti-human CD11b (macrophage marker, Clone# LM2,Cat# 393,107,Dilution#1:20), FITC anti-human CD68 (macrophage marker, Clone#Y1/82A,Cat# 333,805,Dilution#1:20), APC anti-human CD80 (M1 macrophage marker, Clone#2D10, Cat# 305,219, Dilution#1:20), PerCP anti-human CD163 (M2 macrophage marker, Clone#GHI/61, Cat# 333,625, Dilution#1:20), PE anti-human CD206 (M2 macrophage marker, Clone#15–2, Cat# 321,105, Dilution#1:20), and Cyto-Fast Fix/Perm Buffer Set (Cat# 426,803, Dilution#1:9). All antibodies were used at a specification of 25 tests. Single-cell suspensions were prepared, stained with surface antibodies, vortexed, and incubated in the dark. After washing and centrifugation, cells were fixed, permeabilized, and stained with intracellular antibodies if required before acquisition on a flow cytometer. Raw data were analyzed using FlowJo V10 software to calculate the total percentage of macrophages and the proportions of M1 and M2 subtypes.Flow cytometry gating strategy: Within the All Events gate, the single cell population (Gate 2) was gated by the combination of forward scatter area (FSCA) and forward scatter height (FSCH) to remove adherent cells, and the P1 gate was obtained. From the P1 gate, CD68-positive cell populations were identified by SSC and CD68, which were total macrophages, and the P2 gate was obtained. From the P2 gate, CD80+ M1 cell populations and CD163+ M2 cell populations were identified by CD80 and CD163. The remaining antibodies were used to further validate the M1 and M2 cell phenotypes.

For IHC, paraffin-embedded tissue sections were deparaffinized, rehydrated, and subjected to antigen retrieval. After blocking, sections were incubated with primary antibodies, followed by appropriate secondary antibodies and chromogen development. Stained slides were scanned and analyzed using the Aipathwell® AI-powered digital pathology image analysis software to quantify parameters including positive cell rate, positive cell density, H-score, and Immunoreactive Score (IRS). Quantitative scoring criteria for immunohistochemistry: The Aipathwell® digital pathological image analysis software was used for quantitative analysis of immunohistochemical staining results. Staining intensity (SI) was classified into 4 grades: grade 0 (no staining), grade 1 (weak positive, light yellow), grade 2 (moderate positive, brownish yellow), grade 3 (strong positive, tan). The percentage of positive cells (PP) was divided into 5 grades: grade 0 (0–5%), grade 1 (6–25%), grade 2 (26–50%), grade 3 (51–75%), grade 4 (>75%). The final immunoreactive score (IRS) was calculated as SI × PP, with a total score ranging from 0 to 12. Samples with an IRS ≤ 3 were defined as low expression, and those with an IRS > 3 were defined as high expression.

Quantitative real-time PCR (qPCR) and western blot analysis

The human colorectal cancer cell line HCT-116 was used for in vitro experiments. Total RNA was extracted immediately after cell collection. Reverse transcription was performed using the SynScript® III RT SuperMix for qPCR. Subsequent amplification reactions were carried out using the ArtiCanATM SYBR qPCR Mix on a real-time PCR system. Relative gene expression was calculated using the 2^(-ΔΔCt) method: ΔCt was determined by subtracting the Ct value of the reference gene from the Ct value of the target gene; ΔΔCt was then calculated as the difference between the ΔCt of the test sample and the ΔCt of the control sample; finally, the relative quantity (RQ) was derived using the formula $RQ = 2^{(-\Delta\Delta Ct)}$.

For protein analysis, total cellular protein was extracted from adherent HCT-116 cells using a monolayer cell lysis protocol. Protein concentration was determined using a BCA assay. Protein lysates were mixed with 5 × loading buffer, denatured by heating, and separated by SDS-PAGE. Subsequently, proteins were transferred to a membrane for Western blot analysis. Protein bands were visualized, and their grayscale values were quantified using ImageJ software. The expression level of the target protein was normalized to that of the internal control protein.

Statistical analysis

Statistical analysis was performed using SPSS 26.0 software. Continuous data are presented as mean ± standard deviation ($\bar{x} \pm s$). A two-sided p-value < 0.05 was considered statistically significant for all analyses. For paired samples (colorectal cancer tissue [CA group] vs. paired adjacent normal tissue [NOR group]): The Shapiro-Wilk test was first used to test the normality of the paired differences (measured value of cancer tissue - measured value of paired adjacent normal tissue). For paired data with normally distributed differences, a two-tailed paired *t*-test was used for comparison. For paired data with non-normally distributed differences, a two-tailed Wilcoxon signed-rank test was used for comparison. For unpaired two-group comparisons: For data conforming to normal distribution and homogeneity of variance, a two-tailed independent samples *t*-test was used. For data with non-normal distribution, the two-tailed Mann-Whitney U test was used. For comparisons among multiple groups, one-way analysis of variance (ANOVA) was employed, followed by Tukey's post-hoc test for pairwise comparisons.

Results

Survival analysis of the ETV4 gene

The precise mechanisms of ETV4 in colorectal cancer remain incompletely understood. A total of 701 samples from the TCGA public database were analyzed, comprising 51 normal controls and 650 tumor tissues. Analysis of ETV4 expression differences between the disease and control groups revealed that its expression was significantly elevated in tumor tissues (Fig. 1A). Survival analysis, based on grouping patients according to high or low ETV4 expression, demonstrated a significant association with patient prognosis. At the optimal survival cutoff, the high ETV4 expression group showed a significantly poorer overall survival rate ($p = 0.0021$) (Fig. 1B-D).

Univariate and multivariate cox regression analysis and clinical correlation of ETV4

To evaluate the independent prognostic value of ETV4, univariate and multivariate Cox proportional hazards regression models were constructed based on clinical data and ETV4 expression levels, with results visualized using forest plots. Univariate Cox regression analysis identified Age, Stage, T, M, and N as significant risk factors for CRC patients. Subsequent multivariate analysis confirmed Age and T stage as independent risk factors (Fig. 2A-B). Furthermore, we investigated the association between ETV4 expression and various clinical characteristics. The analysis revealed statistically significant correlations between ETV4 expression levels and patient Gender, M stage, and overall Stage (Fig. 2C-I).

Co-expression network of the ETV4 gene

To elucidate the functional network associated with ETV4, a co-expression analysis was performed using the expression profiles of CRC patients from the TCGA database. Genes with an absolute Pearson correlation coefficient > 0.65 and a p-value < 0.05 were considered significantly co-expressed with ETV4. This analysis identified 60 genes whose expression was significantly correlated with ETV4. The top 10 genes exhibiting the strongest positive and negative correlations are displayed in a heatmap (Fig. 3A), while the overall co-expression network is visualized in a correlation circle plot (Fig. 3B).

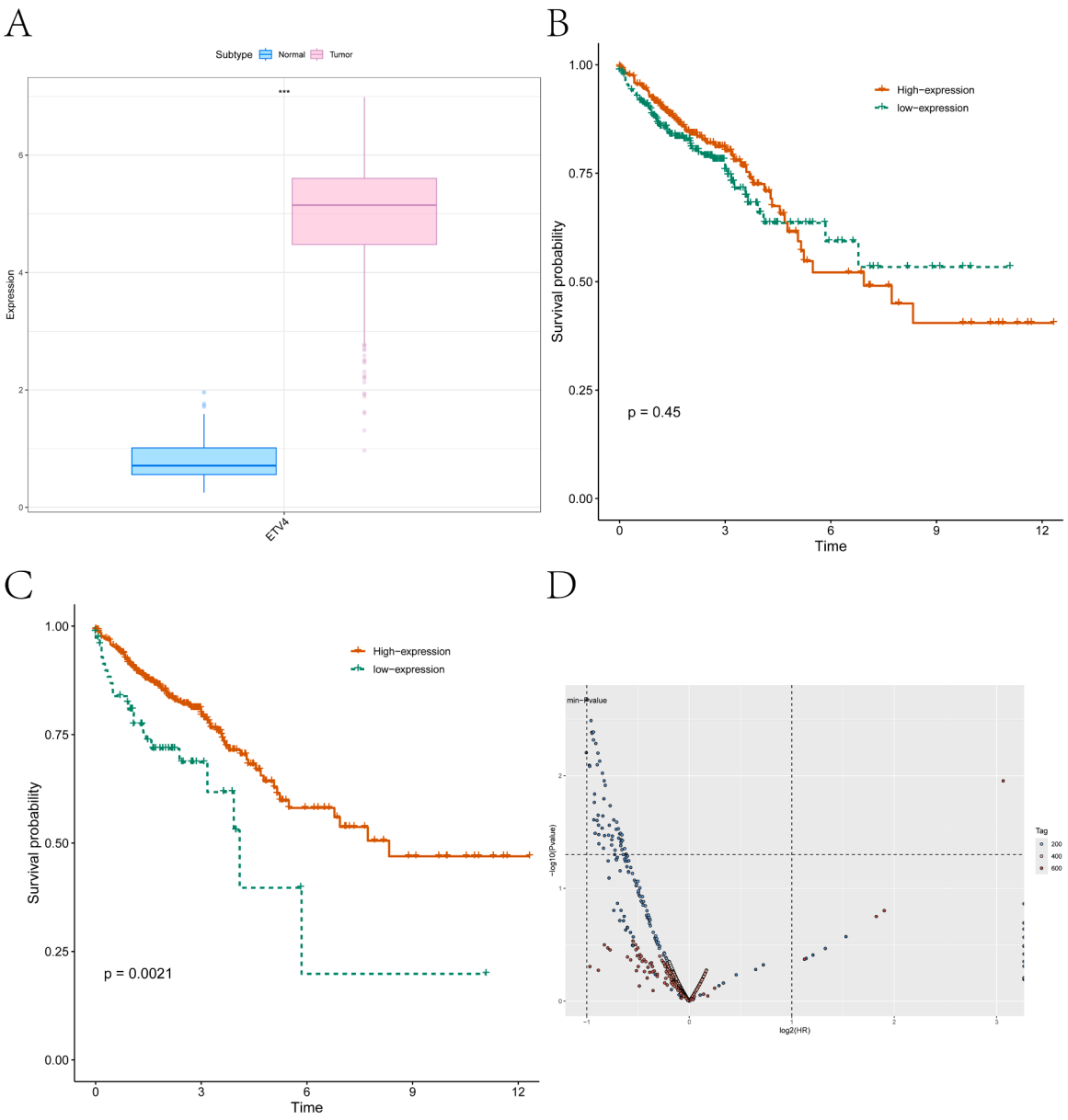

Fig. 1. Survival analysis and expression differential of ETV4 in CRC. (A) Differential expression of the ETV4 gene. Control patients are depicted in blue, and tumor patients in pink. (B) Kaplan-Meier curve showing overall survival of CRC patients stratified by the median expression level of ETV4. (C) Kaplan-Meier curve showing overall survival of CRC patients stratified by the optimal cutoff expression level of ETV4. (D) Forest plot illustrating the association between P-values and hazard ratios for ETV4 expression and other clinical variables.

Immune infiltration analysis

To investigate the relationship between ETV4 and tumor immune infiltration, we analyzed data from the TCGA cohort. The relative proportions of various immune cell types within each patient, as well as the correlations among these immune cells, are presented in different formats (Fig. 4A-B). Comparative analysis revealed significant differences in the infiltration levels of several immune cell subsets between the high and low ETV4 expression groups, including Eosinophils, Macrophages M0, Macrophages M2, resting Mast cells, resting NK cells, Plasma cells, and activated CD4 memory T cells (Fig. 4C). Furthermore, we performed a correlation analysis to directly assess the association between ETV4 gene expression and the abundance of specific immune cell types. The results demonstrated that ETV4 expression showed a significant positive correlation with cells such as activated CD4 memory T cells and Macrophages M0. Conversely, it exhibited significant negative correlations with resting Mast cells and Macrophages M2, among others (Fig. 4D).

Signaling pathways and gene mutations associated with ETV4

To investigate the specific signaling pathways involved and explore the potential molecular mechanisms by which ETV4 influences tumor progression, we performed Gene Set Enrichment Analysis (GSEA). The results indicated that high ETV4 expression was significantly enriched in gene sets related to processes such as the extrinsic apoptotic signaling pathway, intracellular receptor signaling pathway, and regulation of extrinsic apoptotic signaling pathway (Fig. 5A-B), suggesting that ETV4 may affect CRC progression through these mechanisms. Furthermore, Gene Set Variation Analysis (GSVA) revealed enrichment of ETV4-related samples in established oncogenic pathways including *WNT_BETA_CATENIN_SIGNALING* and *MTORC1_SIGNALING* (Fig. 5C).

Single-cell transcriptomic analysis

Single-cell analysis was performed on the GSE231559 dataset using

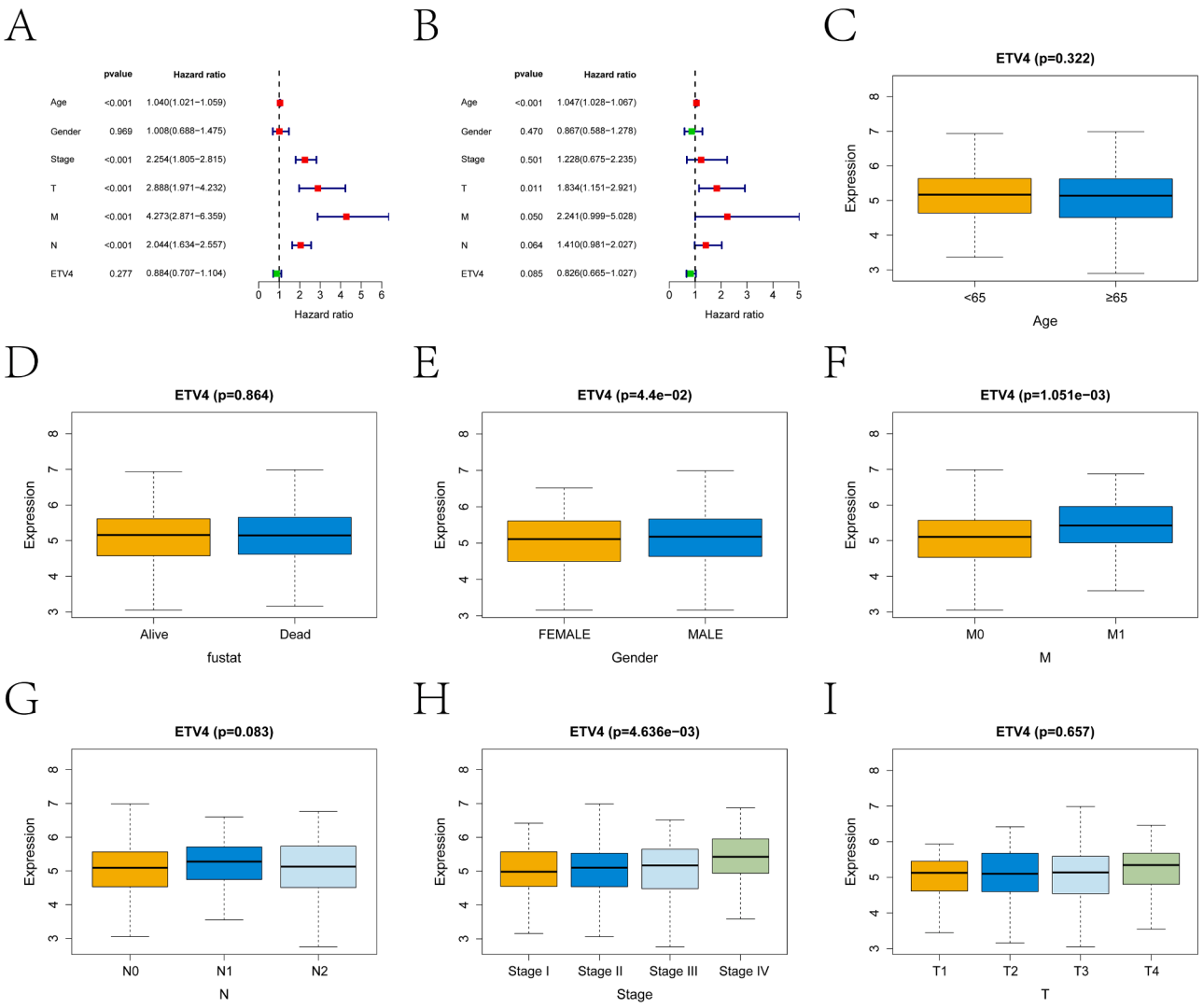

Fig. 2. Univariate/multivariate Cox regression analysis and clinical correlation of ETV4. (A-B) Forest plots of univariate (A) and multivariate (B) Cox proportional hazards regression analyses for ETV4 expression and clinical features. (C-I) Correlation analysis between ETV4 expression and various clinical characteristics, including Gender (C), T stage (D), N stage (E), M stage (F), Stage (G), Age (H), and Tumor status (I). Statistical significance is indicated (*$p < 0.05$, **$p < 0.01$, ***$p < 0.001$).

the Seurat package. Cell clustering via the UMAP algorithm yielded 18 distinct subclusters (Fig. 6A). These clusters were subsequently annotated into 7 major cell types: Epithelial cells, T cells, Monocytes, B cells, Fibroblasts, Plasma cells, and Endothelial cells (Fig. 6B). Furthermore, we analyzed the expression pattern of ETV4 across these annotated cell populations (Fig. 6C-D). To functionally characterize ETV4, we applied the AUCell function to quantify activity scores for gene sets related to immune and metabolic pathways in the single-cell data. A bubble plot visualizing the differential pathway activities revealed that ETV4 was associated with higher activity in pathways such as myc_targets_v1 and myc_targets_v2 (Fig. 6E).

Flow cytometry and immunohistochemistry

Flow cytometric analysis of tissue samples revealed a significantly enhanced polarization towards the M2 macrophage phenotype within tumor tissues compared to adjacent normal tissues (47.68% vs 35.29%, $p = 0.001$), representing a 1.35-fold increase (Fig. 7A). This finding is consistent with a tumor microenvironment that promotes an immunosuppressive, M2-like macrophage polarization. Concurrently, the M1/M2 ratio was markedly decreased in tumor tissues (0.61 vs 1.03, $p < 0.001$), indicative of a significant shift in the local immune balance (Table 1). Analysis correlating these findings with clinical stage demonstrated a positive correlation between advanced T stage (T3/T4 vs. T2) and enhanced M2 polarization, accompanied by a significant reduction in the M1/M2 ratio (Table 2). Immunohistochemical analysis of the same sample cohort confirmed that ETV4 protein expression was substantially higher in tumor tissues than in normal tissues (Fig. 7B).

Validation by quantitative real-time PCR (qPCR) and western blot analysis

Given that the *WNT/β-catenin* signaling pathway is a central driver in colorectal carcinogenesis and our prior GSVA analysis implicated ETV4 in the *WNT_BETA_CATENIN_SIGNALING* pathway, we sought to functionally validate this interaction in vitro. Using specific pharmacological modulators—CHIR99021, an agonist, and XAV939, an inhibitor of the *WNT/β-catenin* pathway—we assessed their effects on ETV4 expression and downstream targets. qPCR analysis demonstrated that, compared to the negative control (NC) group, CHIR99021 treatment significantly increased ETV4 mRNA levels, whereas XAV939 treatment markedly decreased its expression (Fig. 7C). Consistently, Western blot analysis revealed that CHIR99021 significantly upregulated the protein levels of ETV4, nuclear β-Catenin, total β-Catenin, c-Myc, and Cyclin D1. Conversely, XAV939 treatment led to significant suppression of these

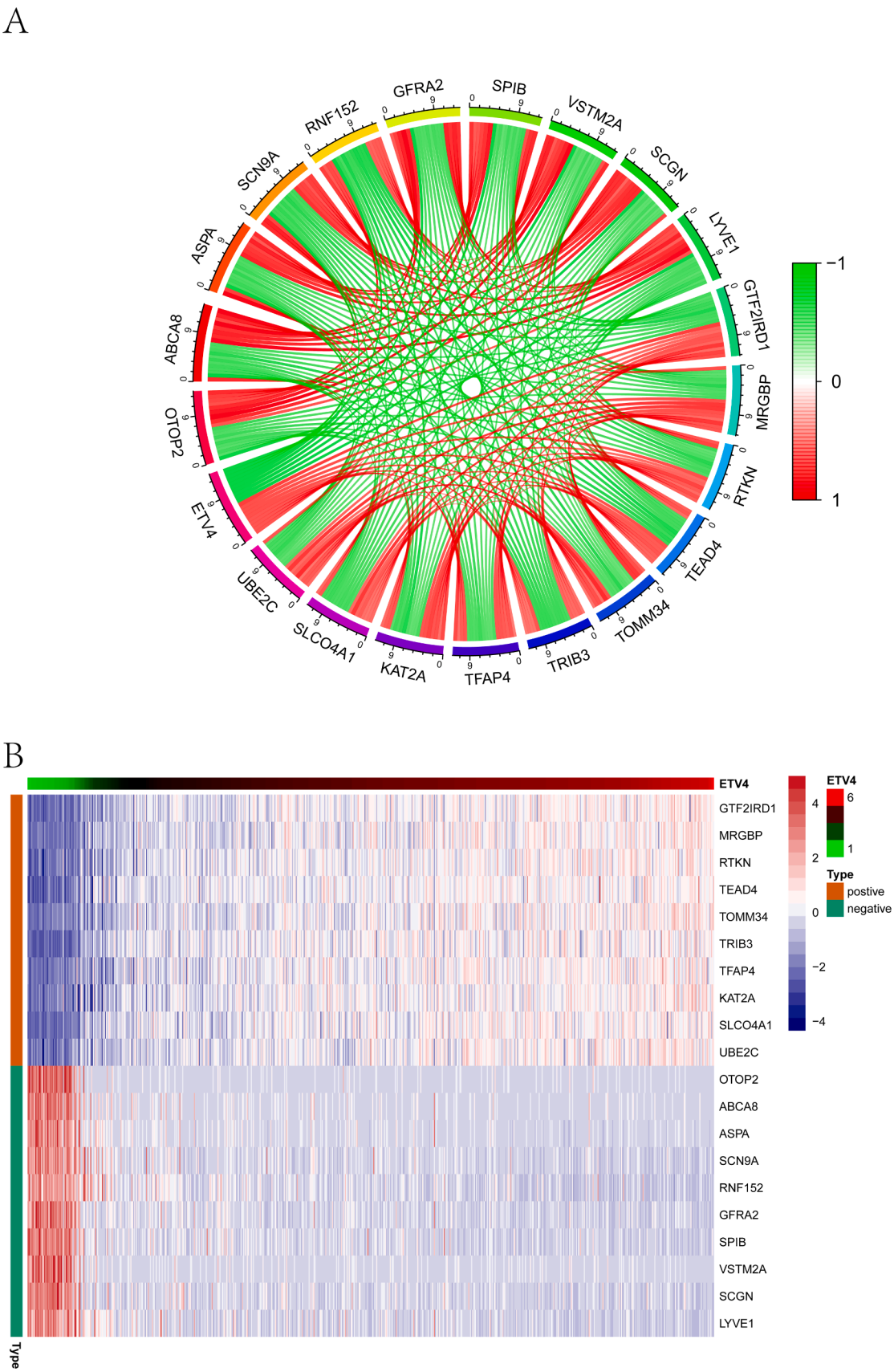

Fig. 3. Co-expression analysis of ETV4. (A) Correlation circle plot of the top 10 genes showing the strongest positive (red) and negative (green) correlation with ETV4 expression. (B) Heatmap displaying the expression levels of the top 10 positively and negatively correlated genes with ETV4 across samples.

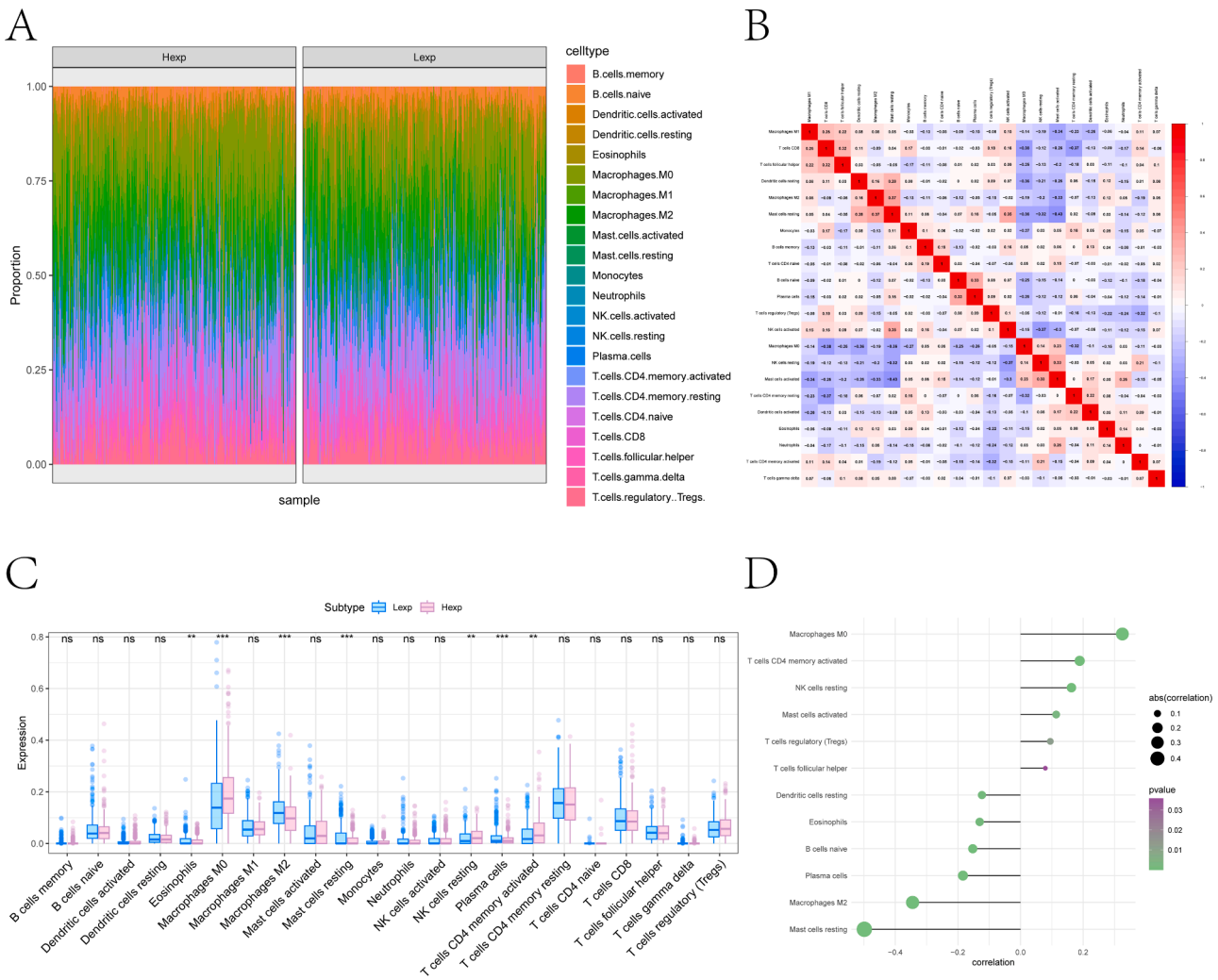

Fig. 4. Analysis of immune cell infiltration. (A) Relative percentages of various immune cell subsets in samples stratified by high (pink) and low (blue) ETV4 expression. (B) Correlation matrix among different immune cell types. Positive correlations are shown in red, and negative correlations in blue. (C) Violin plots showing the differential infiltration levels of specific immune cells between the high and low ETV4 expression groups. (D) Correlation scatter plots depicting the relationship between ETV4 expression levels and the abundance of selected immune cell types.

proteins compared to the NC group (Fig. 7D-E).

Discussion

In recent years, despite significant therapeutic advances with minimally invasive and robotic surgical techniques for colorectal cancer (CRC), the 5-year survival rate for patients with advanced-stage disease remains unsatisfactory. Notably, the incidence of CRC among individuals younger than 50 years is increasing, making it the third leading cause of cancer-related death in this demographic [11]. The introduction of immune checkpoint inhibitors for treating dMMR or MSI-H CRC marks a milestone in immunotherapy [3]. Clinical trials have demonstrated that pembrolizumab (a PD-1 inhibitor) and ipilimumab (a CTLA-4 inhibitor) confer significant therapeutic benefits, including prolonged overall survival (OS) [12,13]. Therefore, in-depth investigation of the immunotherapeutic landscape and its regulatory molecules in CRC holds strong clinical significance for patients with intermediate to advanced disease.

ETV4 is a member of the ETS (E26 transformation-specific) family of transcription factors. Among its family members, ETV4 exhibits the most pronounced alterations in CRC [14]. Its structure contains an ETS domain, which facilitates protein heterodimerization and plays a crucial role in the transcriptional activation of downstream targets [15]. Existing studies have confirmed its high expression and functional involvement in various malignancies, including liver [16], pancreatic [17], and bladder cancers [18]. In contrast, ETV4 is expressed at low or undetectable levels in mature tissues, typically maintained in a self-inhibited state. During development, it plays important roles in angiogenesis, cell cycle control, and apoptosis under physiological conditions, although the specific signaling pathways it regulates remain largely unknown.

In this study, analysis of CRC transcriptomic data revealed that ETV4 is significantly overexpressed in CRC, a finding corroborated by immunohistochemistry. Further survival analysis, stratified by ETV4 expression levels, indicated a negative correlation between high ETV4 expression and patient OS. The tumor immune microenvironment (TIME), comprising diverse immune cells along with molecular and metabolic features, critically influences the effective activation of the immune system by immune checkpoints [19]. Our immune infiltration analysis demonstrated that ETV4 expression positively correlated with activated CD4 memory T cells and M0 macrophages, while negatively correlating with resting mast cells and M2 macrophages. GSVA results indicated enrichment of ETV4-high samples in the *WNT_BETA_CATENIN_SIGNALING* pathway, a core driver of CRC tumorigenesis and progression whose aberrant activation is implicated throughout tumor development [20]. These collective findings suggest that ETV4 is

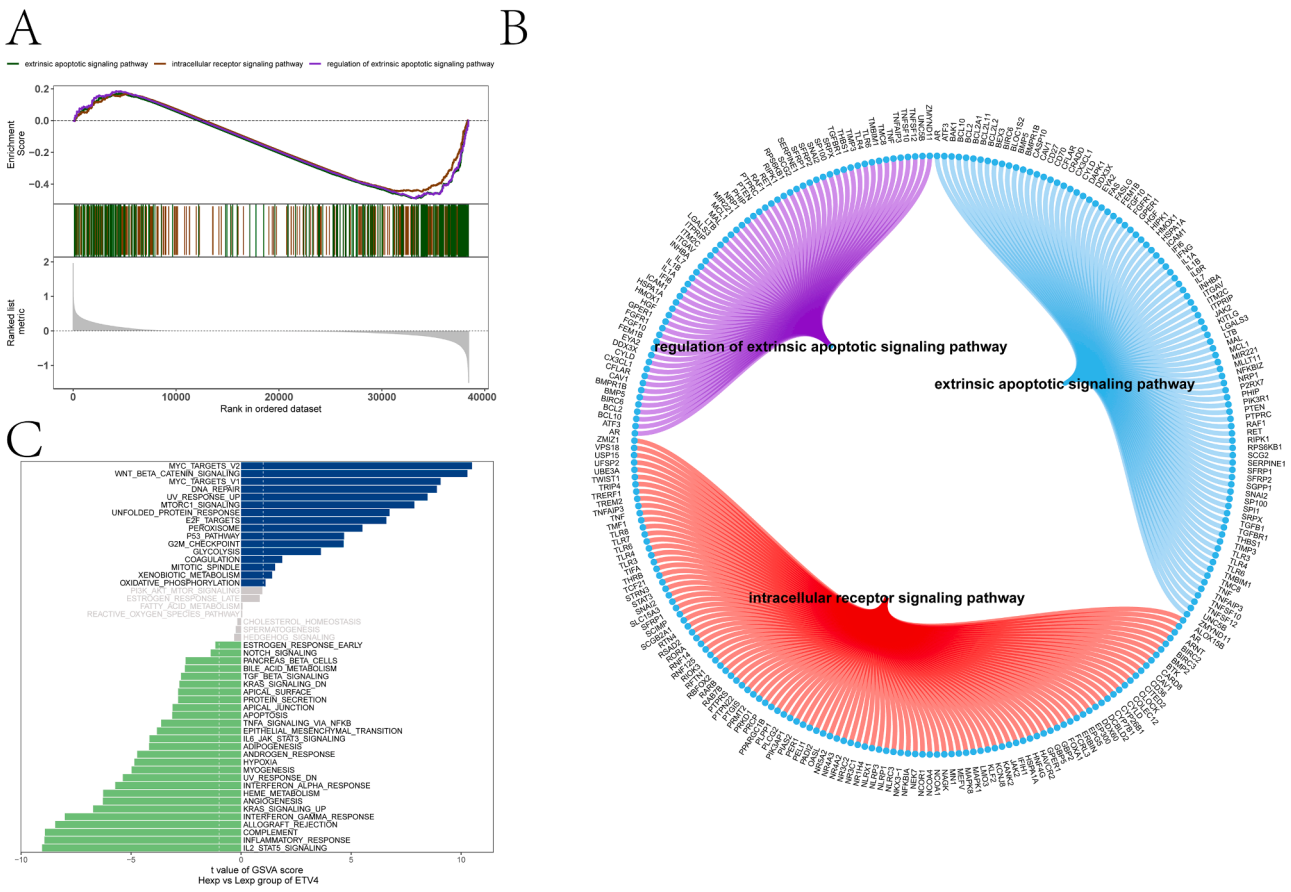

Fig. 5. Gene Set Enrichment Analysis (GSEA) and Gene Set Variation Analysis (GSVA). (A-B) GSEA enrichment plots and leading-edge analysis for ETV4-associated KEGG pathways. (C) GSVA score heatmap showing the enrichment of ETV4-high and ETV4-low samples in hallmark gene sets. Pathways enriched in the low-expression group are marked in green.

involved in regulating CRC pathogenesis.

Flow cytometry confirmed a significantly increased proportion of M2-polarized macrophages in CRC tissues, indicating a shift in the TIME towards a pro-tumorigenic state. Existing research shows that M2 macrophages secrete factors such as IL-10 and TGF-β, which suppress anti-tumor immunity [21,22] and thereby promote CRC progression. Integrated with single-cell analysis, which showed ETV4 expression in T cells and monocytes and its association with high activity in myc_targets_v1/v2 pathways, the correlation between high ETV4 expression and decreased M2-type macrophages suggests that ETV4 may be involved in the regulation of macrophage differentiation. M0 macrophages can differentiate towards an immunosuppressive phenotype [23], and ETV4 may affect this process This speculation remains to be further verified by functional experiments. Significant progress has been made in developing therapies targeting tumor-associated macrophages (TAMs) in CRC [7], as they promote invasion, metastasis, angiogenesis, and mediate immune suppression. As the most abundant immune cell infiltrate in the TIME, TAMs are of paramount importance in CRC. Our flow cytometry experiments provide, to our knowledge, the first direct evidence linking ETV4 to macrophage polarization in CRC, thereby supplementing the molecular mechanisms by which ETS family transcription factors regulate tumor immunity.

GSVA analysis implicated ETV4 in the *WNT_BETA_CATENIN_SIGNALING* pathway. Functional validation via qPCR and Western blot confirmed that the WNT pathway agonist CHIR99021 significantly upregulated ETV4 mRNA and protein expression, whereas the inhibitor XAV939 suppressed it. Furthermore, changes in ETV4 expression positively correlated with levels of nuclear/total β-catenin, c-Myc, and Cyclin D1. These results suggest that ETV4 is likely a downstream target gene of the WNT pathway. Originally identified as a key regulator in Drosophila development [24], the *WNT/β-catenin* pathway, with β-catenin as its central component, is implicated in approximately 90% of CRC cases [25]. Numerous factors influence CRC pathogenesis through this pathway; for instance, secreted protein 62 promotes CRC cell stemness by activating *WNT/β-catenin* signaling [26], while heat shock protein 8 (HSPA8) [27] and the long non-coding RNA NEAT1 [28] facilitate CRC progression and metastasis via Wnt signal activation.

The dysregulation of β-catenin in cancer often manifests more in its aberrant nuclear localization rather than mere expression levels, posing challenges for detection [29]. As a downstream target of the *WNT* pathway, assessing ETV4 expression could serve as a more accessible and reliable surrogate, potentially aiding in earlier clinical diagnosis and treatment evaluation.

In summary, this study demonstrates that ETV4 is overexpressed in CRC and is associated with poor patient prognosis, potentially through mechanisms involving the regulation of immune cell infiltration and the induction of immunosuppressive M2 macrophage polarization. Furthermore, as a key downstream target gene of the *WNT* pathway, ETV4 is widely involved in regulating various biological processes, including CRC cell proliferation and TIME remodeling, highlighting its close association with CRC development and progression. The findings of this study suggest that ETV4 may serve as a potential diagnostic biomarker and candidate therapeutic target for colorectal cancer, providing a new direction for subsequent research on the diagnosis and treatment of colorectal cancer.

However, several limitations of this study should be acknowledged. First, this study is a retrospective analysis with a relatively limited sample size of 40 cases, which may compromise the statistical power of

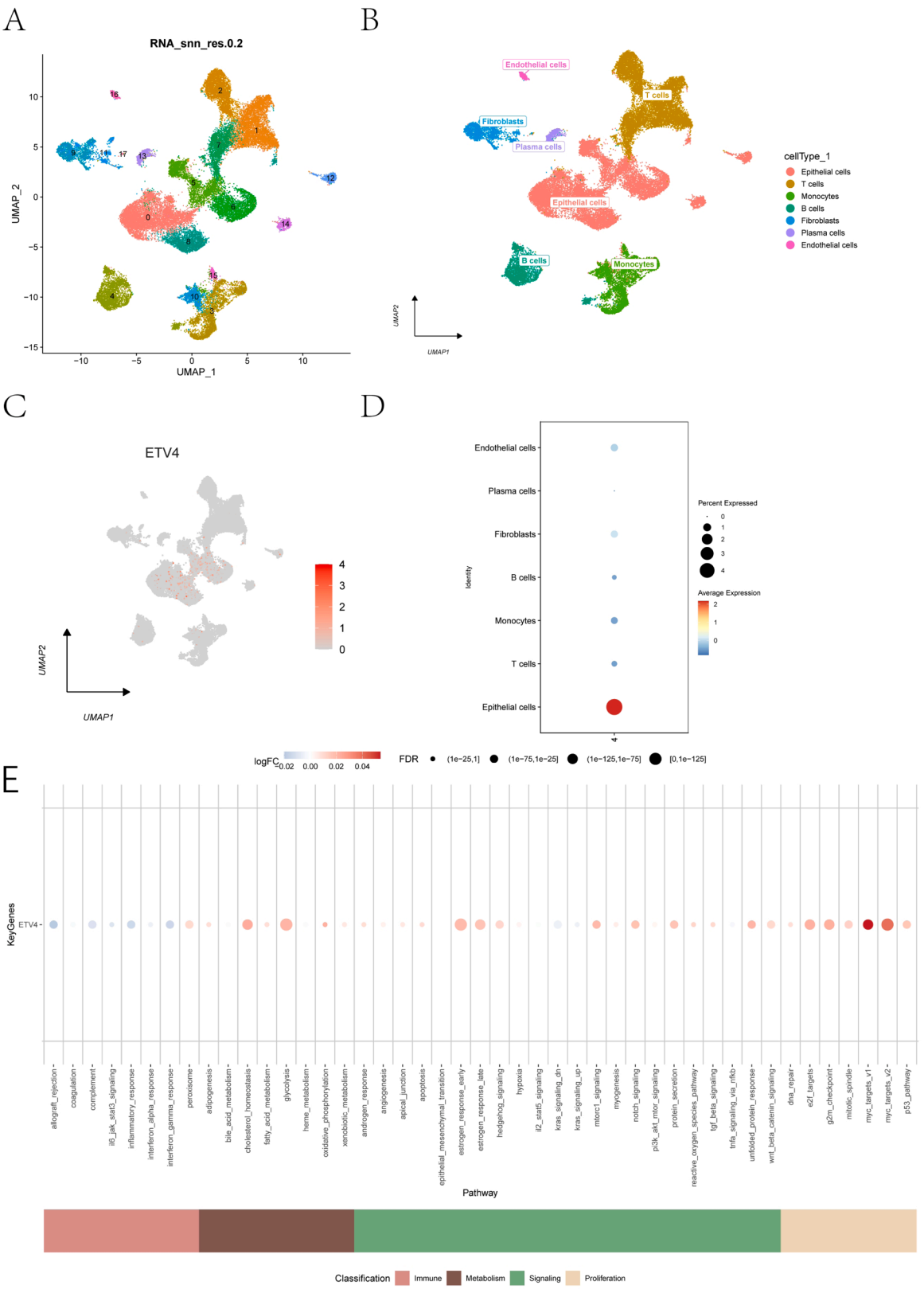

Fig. 6. Single-cell transcriptomic profiling. (A) UMAP projection of single cells from CRC samples, colored by 18 distinct clusters identified via graph-based clustering. (B) UMAP plot showing the annotation of the 18 clusters into 7 major cell types. (C) Scatter plot (UMAP) visualizing the expression levels of ETV4 across all single cells, with expression gradient from blue (low) to red (high). (D) Bubble plot showing the expression distribution profile of transcription factor ETV4 across 7 annotated cell types. The bubble size is proportional to the mean expression level of ETV4 in each cell type, and the color intensity corresponds to the percentage of ETV4-positive cells within each cell type.(E) Bubble plot showing the AUCell activity scores for immune and metabolic pathways in relation to ETV4 expression status. Pathway activity is represented by color gradient from blue (low) to red (high), and the dot size corresponds to the statistical significance.

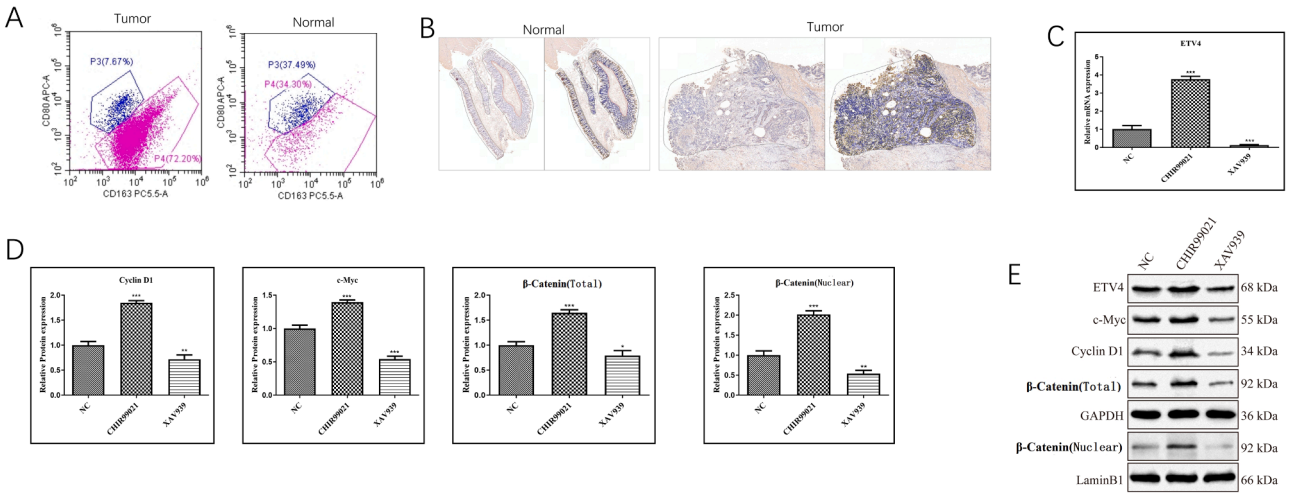

Fig. 7. Flow cytometry and immunohistochemistry validation. (A) Representative flow cytometry plots showing the proportions of M1 and M2 macrophage subsets in tumor tissue and adjacent normal tissue. (B) Representative immunohistochemical (IHC) staining of ETV4 protein in normal colorectal tissue and CRC tissue. (C) Relative mRNA expression levels of ETV4 as determined by qPCR in cells treated with the WNT pathway agonist CHIR99021, inhibitor XAV939, or negative control (NC). (D-E) Representative Western blots and relative densitometric quantification of protein expression levels.

Table 1
Comparison of macrophage subtype distribution between colorectal cancer tissue (CA group) and normal adjacent tissue (NOR group) ($n = 40$).

Parameter	CA Group (Mean ± SD)	NOR Group (Mean ± SD)	Fold Change	Statistic	p-value
Total Macrophages (CD68+, %)	2.13 ± 2.31	1.52 ± 1.38	1.40	Z = 1.71	0.089
M1 Macrophages (CD80+, %)	23.57 ± 12.34	28.62 ± 11.59	0.82	t=−2.28, df=39	0.027*
M2 Macrophages (CD163+, %)	47.68 ± 17.51	35.29 ± 15.86	1.35	t = 3.51, df=39	0.001**
M1/M2 Ratio	0.61 ± 0.45	1.03 ± 0.72	0.59	t=−3.87, df=39	<0.001***

Fold change = Mean value of CA group / Mean value of NOR group; SD = standard deviation, df = degrees of freedom. Normality of paired differences (CA - NOR) was verified by Shapiro-Wilk test. Two-tailed paired *t*-test was used for normally distributed data (M1 Macrophages, M2 Macrophages, M1/M2 Ratio), and two-tailed Wilcoxon signed-rank test was used for non-normally distributed data (Total Macrophages); *$p < 0.05$, **$p < 0.01$, ***$p < 0.001$.

Table 2
Association analysis between tumor stage and macrophage subtypes.

Parameter	T2 Stage (Mean ± SD)	T3/T4 Stage (Mean ± SD)	Statistic	p-value
M2 Macrophages (CD163+, %)	38.75 ± 15.22	51.32 ± 16.89	t = 1.95, df=38	0.018
M1/M2 Ratio	0.85 ± 0.51	0.48 ± 0.32	t = 2.76, df=38	0.009

SD = standard deviation, df = degrees of freedom. Normality and homogeneity of variances were confirmed by Shapiro-Wilk test and Levene's test. Two-tailed independent samples *t*-test was used for inter-group comparisons; $p < 0.05$ was considered statistically significant.

our findings and restrict the generalizability of the conclusions to broader patient cohorts. Second, the regulatory mechanism of ETV4 on the tumor immune microenvironment was only preliminarily explored in this study, and the specific underlying molecular pathways still need further validation. In addition, functional experiments verifying the role of ETV4 in macrophage polarization are lacking, and in vivo validation using animal models to confirm the tumor-promoting effect of ETV4 and its related mechanisms is also absent in the current work. For future research, we will take the functional validation of ETV4 in macrophage polarization as the core priority, and further delve into the molecular interactions between ETV4, the *WNT/β-catenin* pathway, and immune checkpoints, so as to solidify the current conclusions and provide a more robust theoretical foundation for clinical translation and application

Ethics approval and consent to participate

This study was approved by the Ethics Approval Committee at Ordos Central Hospital. Written informed consent was obtained from each study subject.

Data availability

The datasets used and/or analyzed during the current study are available from the corresponding author on reasonable request.

Funding

This work was supported by the Public Hospital Research Collaborative Fund Science and Technology Project (Grant No 2023GLLH0256).

CRediT authorship contribution statement

Ruipeng Meng: Writing – original draft, Data curation. **Shilong Wang:** Software. **Zhanfei She:** Validation. **Huaiming Wang:** Investigation. **Bo Wu:** Investigation. **Yu Qiao:** Data curation. **Pengyuan Chen:** Data curation. **Nargerel:** Data curation. **Xiaofeng Yang:** Data curation. **Liang Wang:** Formal analysis.

Declaration of competing interest

The authors declare that they have no known competing financial interests or personal relationships that could have appeared to influence the work reported in this paper.

References

[1] E. Morgan, M. Arnold, A. Gini, V. Lorenzoni, C.J. Cabasag, M. Laversanne, J. Vignat, J. Ferlay, N. Murphy, F. Bray, Global burden of colorectal cancer in 2020

and 2040: incidence and mortality estimates from GLOBOCAN, Gut 72 (2023) 338–344.
[2] S.G. Patel, J.J. Karlitz, T. Yen, C.H. Lieu, C.R. Boland, The rising tide of early-onset colorectal cancer: a comprehensive review of epidemiology, clinical features, biology, risk factors, prevention, and early detection, Lancet Gastroenterol. Hepatol. 7 (2022) 262–274.
[3] B. Yu, J. Kang, H. Lei, Z. Li, H. Yang, M. Zhang, Immunotherapy for colorectal cancer, Front. Immunol. 15 (2024) 1433315.
[4] J. Li, C. Wu, H. Hu, G. Qin, X. Wu, F. Bai, J. Zhang, Y. Cai, Y. Huang, C. Wang, J. Yang, Y. Luan, Z. Jiang, J. Ling, Z. Wu, Y. Chen, Z. Xie, Y. Deng, Remodeling of the immune and stromal cell compartment by PD-1 blockade in mismatch repair-deficient colorectal cancer, Cancer Cell 41 (2023) 1152–1169, e1157.
[5] A. Lin, J. Zhang, P. Luo, Crosstalk between the MSI status and tumor microenvironment in colorectal cancer, Front. Immunol. 11 (2020) 2039.
[6] A. Nicolini, P. Ferrari, Involvement of tumor immune microenvironment metabolic reprogramming in colorectal cancer progression, immune escape, and response to immunotherapy, Front. Immunol. 15 (2024) 1353787.
[7] J. Otuagomah, A. Newcomb, T. Gwag, S. Wang, CD47: an immunoregulatory nexus in liver and gastrointestinal disorders, eGastroenterology 3 (2025) e100242.
[8] S. Hou, Y. Zhao, J. Chen, Y. Lin, X. Qi, Tumor-associated macrophages in colorectal cancer metastasis: molecular insights and translational perspectives, J. Transl. Med. 22 (2024) 62.
[9] D. Qi, M. Lu, P. Xu, X. Yao, Y. Chen, L. Gan, Y. Li, Y. Cui, X. Tong, S. Liu, J. Zhao, N. Liu, X. Ye, Transcription factor ETV4 promotes the development of hepatocellular carcinoma by driving hepatic TNF-α signaling, Cancer Commun. (Lond) 43 (2023) 1354–1372.
[10] R. Zhang, Y. Peng, Z. Gao, J. Qian, K. Yang, X. Wang, W. Lu, Y. Zhu, D. Qiu, T. Jin, G. Wang, J. He, N. Liu, Oncogenic role and drug sensitivity of ETV4 in human tumors: a pan-cancer analysis, Front. Oncol. 13 (2023) 1121258.
[11] B.J. Kim, M.H. Hanna, Colorectal cancer in young adults, J. Surg. Oncol. 127 (2023) 1247–1251.
[12] A.J. Bullock, B.L. Schlechter, M.G. Fakih, A.M. Tsimberidou, J.E. Grossman, M. S. Gordon, B.A. Wilky, A. Pimentel, D. Mahadevan, A.S. Balmanoukian, R. E. Sanborn, G.K. Schwartz, G.K. Abou-Alfa, N.H. Segal, B. Bockorny, J.C. Moser, S. Sharma, J.M. Patel, W. Wu, D. Chand, K. Rosenthal, G. Mednick, C. Delepine, T. J. Curiel, J. Stebbing, H.J. Lenz, S.J. O'Day, A.B. El-Khoueiry, Botensilimab plus balstilimab in relapsed/refractory microsatellite stable metastatic colorectal cancer: a phase 1 trial, Nat. Med. 30 (2024) 2558–2567.
[13] D. Song, S. Hou, N. Ma, B. Yan, J. Gao, Efficacy and safety of PD-1/PD-L1 and CTLA-4 immune checkpoint inhibitors in the treatment of advanced colorectal cancer: a systematic review and meta-analysis, Front. Immunol. 15 (2024) 1485303.
[14] T. Jiang, X. Liu, H. Liu, K. Du, Y. Wang, H. Fan, Y. Zhang, L. Cui, H. Zhang, C. Zhang, Y. Zhu, Z. Liu, Y. Bu, Y. Lei, ETV4 interacts with LOXL2 to induce epigenetic activation of NID1 during colorectal cancer progression, Int. J. Biol. Sci. 21 (2025) 6674–6696.
[15] B. Kandemir, U. Dag, B. Bakir Gungor, M. Durasi İ, B. Erdogan, E. Sahin, U. Sezerman, I. Aksan Kurnaz, In silico analyses and global transcriptional profiling reveal novel putative targets for Pea3 transcription factor related to its function in neurons, PLoS. One 12 (2017) e0170585.
[16] M. Xie, Z. Lin, X. Ji, X. Luo, Z. Zhang, M. Sun, X. Chen, B. Zhang, H. Liang, D. Liu, Y. Feng, Y. Wang, Y. Li, B. Liu, W. Huang, L. Xia, FGF19/FGFR4-mediated elevation of ETV4 facilitates hepatocellular carcinoma metastasis by upregulating PD-L1 and CCL2, J. Hepatol. 79 (2023) 109–125.
[17] N. Tyagi, S.K. Deshmukh, S.K. Srivastava, S. Azim, A. Ahmad, A. Al-Ghadhban, A. P. Singh, J.E. Carter, B. Wang, S. Singh, ETV4 Facilitates cell-cycle progression in pancreatic cells through transcriptional regulation of cyclin D1, Mol. Cancer Res. 16 (2018) 187–196.
[18] Q. Zhang, S. Liu, H. Wang, K. Xiao, J. Lu, S. Chen, M. Huang, R. Xie, T. Lin, X. Chen, ETV4 Mediated tumor-associated neutrophil infiltration facilitates lymphangiogenesis and lymphatic metastasis of bladder cancer, Adv. Sci. (Weinh) 10 (2023) e2205613.
[19] K. Aliazis, A. Christofides, R. Shah, Y.Y. Yeo, S. Jiang, A. Charest, V.A. Boussiotis, The tumor microenvironment's role in the response to immune checkpoint blockade, Nat. Cancer 6 (2025) 924–937.
[20] H. Zhao, T. Ming, S. Tang, S. Ren, H. Yang, M. Liu, Q. Tao, H. Xu, Wnt signaling in colorectal cancer: pathogenic role and therapeutic target, Mol. Cancer 21 (2022) 144.
[21] Y. Feng, S. Qiao, J. Chen, X. Wen, Y. Chen, X. Song, J. Xu, X. Qiao, J. Yang, S. Zhang, Y. Feng, Y. Gao, M2-Type macrophages and cancer-associated fibroblasts combine to promote colorectal cancer liver metastases, Onco Targets. Ther. 17 (2024) 243–260.
[22] P. Ouyang, K. Li, W. Xu, C. Chen, Y. Shi, Y. Tian, J. Gong, Z. Bao, METTL3 recruiting M2-type immunosuppressed macrophages by targeting m6A-SNAIL-CXCL2 axis to promote colorectal cancer pulmonary metastasis, J. Exp. Clin. Cancer Res. 43 (2024) 111.
[23] A.J. Boutilier, S.F. Elsawa, Macrophage polarization states in the tumor microenvironment, Int. J. Mol. Sci. 22 (2021).
[24] K. Kretzschmar, H. Clevers, Wnt/β-catenin signaling in adult mammalian epithelial stem cells, Dev. Biol. 428 (2017) 273–282.
[25] M. Bienz, H. Clevers, Linking colorectal cancer to wnt signaling, Cell 103 (2000) 311–320.
[26] X. Liu, K. Su, X. Sun, Y. Jiang, L. Wang, C. Hu, C. Zhang, M. Lu, X. Du, B. Xing, Sec62 promotes stemness and chemoresistance of human colorectal cancer through activating wnt/β-catenin pathway, J. Exp. Clin. Cancer Res. 40 (2021) 132.
[27] B. Li, H. Ming, S. Qin, L. Zhou, Z. Huang, P. Jin, L. Peng, M. Luo, T. Zhang, K. Wang, R. Liu, Y.C. Liou, E.C. Nice, J. Jiang, C. Huang, HSPA8 Activates wnt/β-catenin signaling to facilitate BRAF V600E colorectal cancer progression by CMA-mediated CAV1 degradation, Adv. Sci. (Weinh) 11 (2024) e2306535.
[28] M. Zhang, W. Weng, Q. Zhang, Y. Wu, S. Ni, C. Tan, M. Xu, H. Sun, C. Liu, P. Wei, X. Du, The lncRNA NEAT1 activates wnt/β-catenin signaling and promotes colorectal cancer progression via interacting with DDX5, J. Hematol. Oncol. 11 (2018) 113.
[29] S. Li, M. Huang, Q. Liu, D. Wang, R. Wu, X. Zhang, W. Chen, L. Duan, Serum expression of β-catenin is a potential detection marker in patients with colorectal cancer, Dis. Markers 2019 (2019) 5070524.